

Multiple Glasses in Asymmetric Binary Hard Spheres

Th. Voigtmann

*Institut für Materialphysik im Weltraum, Deutsches Zentrum für Luft- und Raumfahrt (DLR), 51170 Köln, Germany
Fachbereich Physik, Universität Konstanz, 78457 Konstanz, Germany and
Zukunftskolleg, Universität Konstanz, 78457 Konstanz, Germany*

(Dated: February 15, 2022)

Multiple distinct glass states occur in binary hard-sphere mixtures with constituents of very disparate sizes according to the mode-coupling theory of the glass transition (MCT), distinguished by considering whether small particles remain mobile or not, and whether small particles contribute significantly to perturb the big-particle structure or not. In the idealized glass, the four different glasses are separated by sharp transitions that give rise to higher-order transition phenomena involving logarithmic decay laws, and to anomalous power-law-like diffusion. The phenomena are argued to be expected generally in glass-forming mixtures.

PACS numbers: pacs tbd

Many glass formers and virtually all simple model systems for slow dynamics are mixtures of some sort. Close to a glass transition generic mixing effects appear, such as dramatic changes in viscosity induced by small composition changes [1, 2], that are relevant for applications and may help to shed light on the microscopic processes driving glass formation.

Even more interesting is the possibility to form qualitatively distinct types of glass, depending on mixture composition and constituents. Taking for example binary mixtures with sufficiently disparate constituents, a glass can form where some (slow) species freeze, but a fast component is able to diffuse through the voids left in the amorphous packing. This scenario is particularly relevant for transport through heterogeneous disordered media [3–7] or glassy ion conductors [8, 9]. The simplest model are binary hard-sphere mixtures with large size disparity, where experiments on colloidal suspensions indeed found, depending on relative concentration, a partially frozen “single glass” with mobile small particles, separate from a “double glass” where both particle species freeze [10, 11]. In mixtures of star polymers [12–14] yet another kind of glass emerged, termed “asymmetric” because it is characterized by few big particles frozen in a small-particle matrix, rendering the big-particle nearest-neighbor cages highly nonspherical. It was, however, argued to be a hallmark of the ultra-soft interactions typical for the star polymers.

Another kind of glass intuitively argued for is the “attractive glass” famous from colloid–polymer mixtures where free polymer induces depletion attraction among the colloids. If that attraction is weak, the glass that forms is essentially hard-sphere like or “repulsive”, while at sufficiently strong and short-ranged attraction, a new glass driven by bonding and not nearest-neighbor caging appears. Based on extensively tested predictions of the mode-coupling theory of the glass transition (MCT) for a square-well model system [15–20], one expects the two glasses to be separated by a glass–glass transition

crossing which, for example, the elastic moduli of the glass exhibit sharp changes. Considering the generality of the depletion-interaction mechanism [21], one may indeed expect a similar glass–glass transition to be present in binary mixtures quite generically (lest the relevant parameter space cannot be explored). As such transitions typically involve endpoint singularities that give rise to universal logarithmic decay laws for the time-dependent correlation functions [22], one anticipates regions of mixture composition where these peculiar decay laws can be found. Indeed, they have been reported in computer simulation of soft-sphere mixtures [23].

Here I demonstrate, that already the simplest glass-forming mixture model, the binary hard-sphere mixture, allows to identify *four* qualitatively different glassy states separated by well-defined transitions. The transition diagram lends itself to an intuitive classification: one has to distinguish (i) whether small particles remain mobile in the glass or not, and (ii) whether the structure of the big-particle glass is or is not significantly disturbed by the small particles. Combining these two choices each gives four possible types of glass.

Calculations are based on MCT supplemented by the Percus-Yevick (PY) approximation for the static structure factor [24–26], but following the physically plausible classification, the results can be expected to hold rather generally for binary mixtures whose parameters can be tuned widely enough. The possible interplay with equilibrium phases is ignored here. The resulting glass-transition diagram is a unique prediction of MCT, distinct from other theories that have been put forward [27], and testable in simulation or experiment.

Numerical calculations follow the method of Ref. [25]. MCT takes partial static structure factors $S_{\alpha\beta}(q) = \langle \varrho_{\alpha}^*(\vec{q}) \varrho_{\beta}(\vec{q}) \rangle$ as input (Greek indices label species, and static triplet correlations are neglected here). Here $\langle \cdot \rangle$ is the canonical average, and $\varrho_{\alpha}(\vec{q}) = \sum_k \exp[i\vec{q}\vec{r}_{k,\alpha}]$ is the number-density fluctuation of species α (the sum runs over all particle positions \vec{r} of that type). MCT

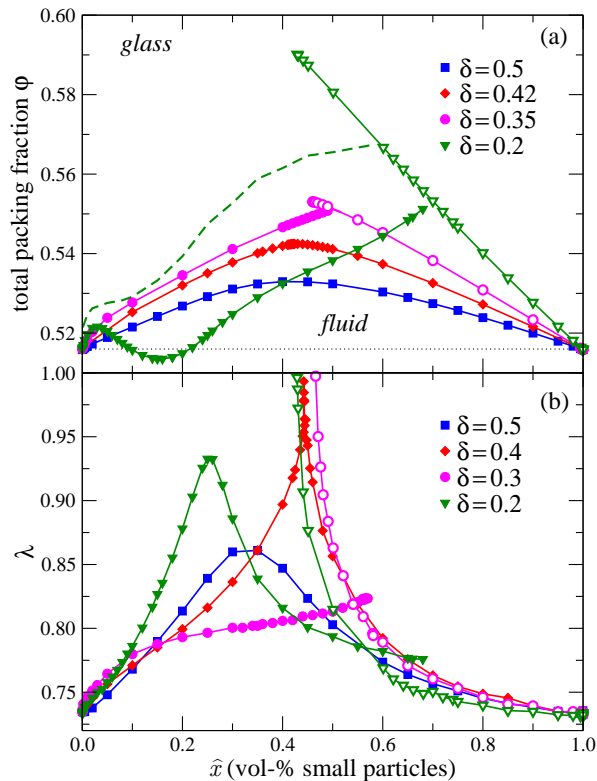


FIG. 1. (a) Glass transition diagram for a model binary hard-sphere mixture obtained from mode-coupling theory. Solid lines show the glass-transition packing fraction $\varphi_c(\delta, \hat{x})$ as a function of small-particle volume concentration, \hat{x} , for various size ratios δ as indicated. The dashed line indicates a separate localization transition $\varphi_c^s(\delta, \hat{x})$ for the small species for $\delta = 0.2$. (b) MCT exponent parameter $\lambda(\hat{x})$ for cuts of constant δ . Solid and open symbols refer to the small- \hat{x} and large- \hat{x} branches, respectively.

predicts collective dynamical density correlation functions $\Phi_{\alpha\beta}(q, t) = \langle \varrho_\alpha^*(\vec{q}, t) \varrho_\beta(\vec{q}) \rangle$, where the time evolution is given by the implicit dependence of $\varrho_\alpha(\vec{q})$ on the trajectories. The long-time limit of that matrix, $\mathbf{F}(q) = \lim_{t \rightarrow \infty} \Phi(q, t)$, distinguishes ergodic liquid states, $\mathbf{F}(q) = \mathbf{0}$, from nonergodic ones, where the correlation matrix decays not to zero but to a positive definite matrix, $\mathbf{F}(q) \succ \mathbf{0}$. Such states are identified as (idealized) glasses within MCT. Standard MCT glass transitions are characterized as bifurcations of the \mathcal{A}_2 type where $\mathbf{F}(q)$ jumps discontinuously. Note that such jumps can also occur inside the glass. The $\mathbf{F}(q)$ can be found numerically [28] on a finite wave-number grid, $q_i = (i+1/2)\Delta q$ with $i = 1, \dots, N = 500$ and $\Delta q = 0.4$ for most calculations here. Small size ratios require higher large- q cutoff, $N = 1000$ was hence used for $\delta < 0.2$.

Results are reported as cuts through the parameter space at constant size ratio $\delta = d_s/d_l \leq 1$, where d_α are the hard-sphere diameters ($\alpha = s, l$ for small and large). The two remaining parameters then are the number densities ρ_α , conveniently expressed as a total packing frac-

tion of the spheres, $\varphi = \sum_\alpha \varphi_\alpha = (\pi/6) \sum_\alpha \rho_\alpha d_\alpha^3$, and a concentration (by volume) of small spheres, $\hat{x} = \varphi_s/\varphi$. To top panel of Fig. 1 illustrates the glass-transition diagram for size ratios $0.2 \leq \delta \leq 0.5$; larger δ are topologically the same as $\delta = 0.5$ [25]. For all compositions at fixed $\delta \gtrsim 0.42$, the binary-mixture glass is separated from the liquid by a smooth line of ordinary \mathcal{A}_2 transitions. In contrast, the curve for, say, $\delta = 0.35$ demonstrates the emergence of a glass-glass transition: the liquid-glass transition splits into two lines that no longer join smoothly, but cross discontinuously at some point, at which one of the lines stops. The other continues inside the glass until it terminates (the corresponding jump in $\mathbf{F}(q)$ disappears) at a higher-order transition point of type \mathcal{A}_3 . The glass-glass transition signals that there are two competing arrest mechanisms at work: caging can either be dominated by large particles or by small ones. As soon as the ratio of relevant length scales (essentially δ) becomes sufficiently distinct from unity, the two mechanisms give rise to glasses with differing intrinsic scales (the localization length, or typical cage size) such that a sharp distinction becomes possible. As pointed out, one way to distinguish these glasses experimentally would be a marked difference in elastic properties. The structure of the large- \hat{x} glass bears resemblance to certain types of sweets [27] such as Italian torroncino. The distinction is only strict for size ratios $\delta < \delta_c$. At δ_c , the glass-glass transition endpoint coincides with the crossing, resulting in an \mathcal{A}_4 singularity. Mathematically, these higher-order singularities are identical to those in one-component descriptions of colloid-polymer mixtures [22], and the same kind of asymptotic expansions predicting the appearance of logarithmic decay laws and their precursors apply here, too. In the present calculations, $\delta_c \approx 0.41$. Since the states $\hat{x} = 0$ and $\hat{x} = 1$ are identical up to a rescaling of lengths with δ , the \mathbf{F} -versus- q curve is broader for $\hat{x} \rightarrow 1$ than for $\hat{x} \rightarrow 0$, and generically higher at fixed q . Hence the large- \hat{x} portion of the transition extends into and demarks the mechanically stiffer glass.

The position of higher-order singularities is revealed by looking at MCT's exponent parameter λ . To each transition point, a particular value of $0.5 \leq \lambda \leq 1$ is assigned in the theory, which determines the power-law exponents valid for the asymptotic expansion of correlation functions close to the transition. At $\lambda = 1$, these power laws cease to be valid and are replaced by logarithmic laws. As seen in the lower panel of Fig. 1, the values of λ indeed rise to unity when approaching the endpoints of the large- \hat{x} glass-transition lines. At $\delta > \delta_c$, λ still rises as a precursor corresponding to a notable decrease in the asymptotic exponents; at $\delta = \delta_c$, the $\lambda(\hat{x})$ -curve reaches unity for the first time before splitting into two branches.

MCT predicts that at all the \mathcal{A}_ℓ transition points discussed so far, all collective partial-density correlation functions show a simultaneous jump in their long-time limits and hence all are nonergodic [28]. However,

this does not need to hold for the nonergodicity factors $f_\alpha^s(q) = \lim_{t \rightarrow \infty} \phi_\alpha^s(q, t)$ associated with the self-motion of the species α , $\phi_\alpha^s(q, t) = \langle \exp[iq(\vec{r}_{s,\alpha}(t) - \vec{r}_{s,\alpha}(0))] \rangle$. $f_s^s(q)$ can remain zero when crossing the glass transition line, if the small particles are below a certain size δ_c^s [29, 30]. A dashed line in Fig. 1(a) demarcates for $\delta = 0.2$ the region where $f_s^s(q) = 0$ and hence the “single glass”. The collective small–small density correlation function remains nonergodic also in the single glass, in distinct disagreement with the SCGLE theory of Ref. [27].

The nature of the transition lines shown in dashed in Fig. 1 is notably different from the \mathcal{A}_ℓ glass transition lines shown as solid lines: they are so-called type A or localization transitions, where the nonergodicity factor $f_s^s(q)$ rises continually from zero upon crossing the transition, as opposed to exhibiting a finite jump. This reflects the different nature of the two transition mechanisms: while ordinary glass transitions are driven by collective caging on local length scales, the localization transition contains a divergent two-point length scale (the localization length of the small particles). This also means that the applicability of MCT to such transitions can be debated (even more than MCT is usually debated). The dashed line in Fig. 1(a) is to be seen as a good qualitative approximation to the localization line [31], as it is expected on physical grounds: increasing the density of the single glass, one will eventually reach a regime where the small particles either have too little void space to move, or are dense enough to form a glass on their own. For this reason, the single-glass region is bounded from below by the liquid-glass transition, from above by a localization transition, and bounded from the high- \hat{x} side by the glass–glass transition in Fig. 1(a). This is in variance with Ref. [27], where no glass–glass transition is found. The separate localization transition in our calculation occurs only below some size ratio δ_c^s strictly smaller than the δ_c where the higher-order singularity first occurs. The precursor to the localization transition is anomalous diffusion in the sense that the small-particle mean-squared displacement, $\delta r^2(t) = \langle (\vec{r}_{s,s}(t) - \vec{r}_{s,s}(0))^2 \rangle$, exhibits power-law growth $\delta r^2(t) \propto t^y$ with an exponent $y < 1$ [29], instead of ordinary diffusion ($y = 1$), or the two-step glass-transition pattern comprising an intermediate plateau ($y \approx 0$). This allows the existence of the “double-transition” scenario to be established, as done recently for simulations of a soft-sphere mixture [9].

So far, we have found three distinct glasses separated by well-defined transitions. The glass–glass transition is similar to the one found in colloid–polymer mixtures: both share the same mathematics, and both arise from a competition of arrest mechanisms on two sufficiently distinct length scales. Tempting as it may be [32], the analogy is flawed, since in the colloid–polymer mixture the small component is always assumed to remain mobile, whereas at the glass–glass transition in Fig. 1 the small component itself becomes the main glass former.

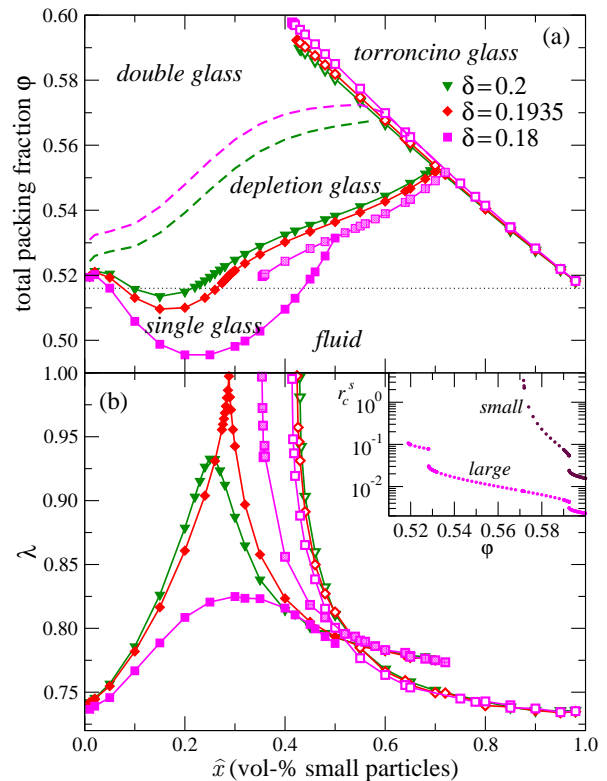


FIG. 2. Transition diagram as in Fig. 1, but for smaller δ . Open, filled, and shaded symbols correspond to $\lambda(\hat{x})$ for the small- \hat{x} , large- \hat{x} , and intermediate- \hat{x} branch of $\phi^c(\hat{x})$, respectively. Inset: localization length $r_{c,\alpha}^s$ for large and small particles for $(\delta, \hat{x}) = (0.18, 0.45)$ as a function of packing fraction.

The analog of the attractive glass in the binary mixture has to be found inside the single glass region. Indeed, extending Fig. 1 to smaller δ , Fig. 2, a second glass–glass transition emerges: a second \mathcal{A}_4 point at roughly $\delta^* = 0.194$ marks the onset of the higher-order singularity scenario for $\delta < \delta^*$ at around $\hat{x} \approx 0.3$. Again, it indicates the discontinuous change of a big-particle dominated glass to one where the small particles set a relevant length scale, but now in the sense that the small particles induce a strong depletion attraction while themselves remaining mobile.

The different glasses are distinguished by the localization lengths $r_{c,\alpha}^s$ of big and small particles – a measure of their cage size. The inset of Fig. 2(b) shows $r_{c,\alpha}^s(\phi)$ along a cut crossing all four transitions. As the repulsive single-glass is first entered, $r_{c,1}^s \approx 0.1$, the Lindemann length for big particles. It discontinuously drops by about δ entering the attractive single-glass, as depletion forces move the large particles closer together. The small-particle $r_{c,s}^s$ remains infinite up to the localization transition, and shows signs of a continuous divergence there (where $r_{c,1}^s$ is smooth). As the “torroncino” glass is entered, both $r_{c,\alpha}^s$ drop discontinuously again, and $r_{c,s}^s \approx 0.1\delta$ indicates a small-particle glass.

To summarize, four different glasses are predicted to form in the simplest model of glass-forming mixtures, viz., binary hard-sphere mixtures, if both composition and size ratio are changed. The four glasses come in two categories, one (“double glass”) where both species freeze simultaneously, and one (“single glass”) where the smaller component remains mobile inside the frozen environment. Each of these comes in two variants, “repulsive” and “attractive”, depending on whether the structure is primarily driven by large-particle caging, or by the small-particle induced forces (be they arrested or not). The attractive double glass naturally explains low-big-particle coordination “asymmetric” cages thought to arise from ultra-soft potentials. Our calculations make it plausible to expect the existence of four glasses much more generically, as long as the relevant mixture parameters cover a sufficiently wide range of states (which may, for example, also depend on dimensionality [26]).

A unique prediction is that the four types of glass are separated by sharp transitions and accompanied by regions in parameter space where signatures of higher-order singularities or of anomalous diffusion may be seen. The latter was found in recent simulations [9]. Features of logarithmic decay that likely are the signature of the first set of \mathcal{A}_3 singularities have been reported [23]. The possibility of attractive glasses emerging around $\delta \approx 0.2 \approx \delta^*$ has been hinted at [33]. Further simulations and experiments are called for to conclusively test our predictions.

Cautionary remarks should be added: first, the PY approximation has known defects. Still it appears to predict $\mathcal{S}(q)$ surprisingly sensibly [34]. The effects discussed above arise from an interplay of different length scales; this should be captured qualitatively correctly in PY. Second, experiment and simulation may require to resort to more complicated interaction potentials, to suppress equilibrium phase transitions that could otherwise interfere. Finally, MCT is driven to a regime where it may likely fail; our predictions thus pose a demanding test case for the theory.

This work was funded by the Helmholtz-Gemeinschaft (HGF), Young Investigator Group VH-NG 406, and the Zukunftscolleg, Universität Konstanz. I thank Emanuela Zaccarelli for insightful cooperation and acknowledge discussion with Jürgen Horbach and Simon Schnyder.

[1] S. R. Williams and W. van Meegen, Phys. Rev. E **64**, 041502 (2001).
 [2] G. Foffi, W. Götze, F. Sciortino, P. Tartaglia, and Th. Voigtmann, Phys. Rev. Lett. **91**, 085701 (2003).
 [3] V. Krakoviack, Phys. Rev. Lett. **94**, 065703 (2005).
 [4] V. Krakoviack, J. Phys.: Condens. Matter **17**, S3565 (2006).
 [5] J. Kurzydum, D. Coslovich, and G. Kahl, Phys. Rev. Lett. **103**, 138303 (2009).

[6] K. Kim, K. Miyazaki, and S. Saito, EPL **88**, 36002 (2009).
 [7] F. Höfling, T. Franosch, and E. Frey, Phys. Rev. Lett. **96**, 165901 (2006).
 [8] Th. Voigtmann and J. Horbach, Europhys. Lett. **74**, 459 (2006).
 [9] Th. Voigtmann and J. Horbach, Phys. Rev. Lett. **103**, 205901 (2009).
 [10] A. Imhof and J. K. G. Dhont, Phys. Rev. Lett. **75**, 1662 (1995).
 [11] A. Imhof and J. K. G. Dhont, Phys. Rev. E **52**, 6344 (1995).
 [12] E. Zaccarelli, C. Mayer, A. Asteriadi, C. N. Likos, F. Sciortino, J. Roovers, H. Iatrou, N. Hadjichristidis, P. Tartaglia, H. Löwen, et al., Phys. Rev. Lett. **95**, 268301 (2005).
 [13] C. Mayer, E. Stiakakis, E. Zaccarelli, C. N. Likos, F. Sciortino, P. Tartaglia, H. Löwen, and D. Vlassopoulos, Rheol. Acta **46**, 611 (2007).
 [14] C. Mayer, E. Zaccarelli, E. Stiakakis, C. N. Likos, F. Sciortino, A. Munam, M. Gauthier, N. Hadjichristidis, H. Iatrou, P. Tartaglia, et al., Nature Materials **7**, 780 (2008).
 [15] W. Götze, *Complex Dynamics of Glass-Forming Liquids* (Oxford University Press, 2009).
 [16] K. Dawson, G. Foffi, M. Fuchs, W. Götze, F. Sciortino, M. Sperl, P. Tartaglia, Th. Voigtmann, and E. Zaccarelli, Phys. Rev. E **63**, 011401 (2001).
 [17] K. N. Pham, A. M. Puentes, J. Bergenholtz, S. U. Egelhaaf, A. Moussaïd, P. N. Pusey, A. B. Schofield, M. E. Cates, M. Fuchs, and W. C. K. Poon, Science **296**, 104 (2002).
 [18] K. N. Pham, S. U. Egelhaaf, P. N. Pusey, and W. C. K. Poon, Phys. Rev. E **69**, 011503 (2004).
 [19] F. Sciortino, P. Tartaglia, and E. Zaccarelli, Phys. Rev. Lett. **91**, 268301 (2003).
 [20] E. Zaccarelli, G. Foffi, F. Sciortino, and P. Tartaglia, Phys. Rev. Lett. **91**, 108301 (2003).
 [21] S. Asakura and F. Oosawa, J. Polym. Sci. **33**, 183 (1954).
 [22] M. Sperl, Phys. Rev. E **68**, 031405 (2003).
 [23] A. J. Moreno and J. Colmenero, J. Chem. Phys. **125**, 164507 (2006).
 [24] W. Götze, in *Amorphous and Liquid Materials*, edited by E. Lüscher, G. Fritsch, and G. Jacucci (Nijhoff, Dordrecht, 1987), vol. 118 of *NATO ASI E: Applied Physics*, pp. 34–81.
 [25] W. Götze and Th. Voigtmann, Phys. Rev. E **67**, 021502 (2003).
 [26] D. Hajnal, J. M. Brader, and R. Schilling, Phys. Rev. E **80**, 021503 (2009).
 [27] R. Juárez-Maldonado and M. Medina-Noyola, Phys. Rev. E **77**, 051503 (2008).
 [28] T. Franosch and Th. Voigtmann, J. Stat. Phys. **109**, 237 (2002).
 [29] L. Sjögren, Phys. Rev. A **33**, 1254 (1986).
 [30] J. Bosse and J. S. Thakur, Phys. Rev. Lett. **59**, 998 (1987).
 [31] S. Schnyder, Diploma thesis, Universität Konstanz (2010).
 [32] R. Juárez-Maldonado and M. Medina-Noyola, Phys. Rev. Lett. **101**, 267801 (2008).
 [33] Ph. Germain and S. Amokrane, Phys. Rev. Lett. **102**, 058301 (2009).
 [34] E. Zaccarelli, private communication.